A clear view of the multifaceted dayside ionosphere of Mars

Paul Withers,[1] Kathryn Fallows,[1] Zachary Girazian,[1] Majd Matta,[1] Bernd Häusler,[2] David Hinson,[3] Len Tyler,[3] David Morgan,[4] Martin Pätzold,[5] Kerstin Peter,[5] Silvia Tellmann,[5] Javier Peralta,[6] and Oliver Witasse[7]

[1] By examining electron density profiles from the Mars Express Radio Science Experiment MaRS, we show that the vertical structure of the dayside ionosphere of Mars is more variable and more complex than previously thought. The top of the ionosphere can be below 250 km (25% occurrence rate) or above 650 km (1%); the topside ionosphere can be well-described by a single scale height (10%) or two/three regions with distinct scale heights (25% or 10%), where those scale heights range between tens and hundreds of kilometers; the main layer of the ionosphere can have a sharply pointed (5%), flat-topped (6%), or wavy (8%) shape, in contrast to its usual Chapman-like shape; a broad increase in electron density is detected at 160–180 km (10%); a narrow increase in electron density is sometimes found in strongly-magnetized regions; and an additional layer is present between the M1 and M2 layers (3%). **Citation:** Withers, P., et al. (2012), A clear view of the multifaceted dayside ionosphere of Mars, *Geophys. Res. Lett.*, *39*, L18202, doi:10.1029/2012GL053193.

1. Introduction

[2] The Martian ionosphere is affected by solar wind conditions, solar extreme-ultraviolet (EUV) and X-ray irradiance, precipitation of charged particles, solar zenith angle, neutral density, composition, and winds, and the magnetic environment. Interactions of the solar wind with inhomogeneous crustal fields are a major cause of spatial and temporal variations in ionospheric chemistry, dynamics, and energetics [*Shinagawa*, 2000; *Connerney et al.*, 2001; *Nagy et al.*, 2004; *Brain*, 2006; *Withers*, 2009]. Understanding the vertical structure of the Martian ionosphere has been a key tool for discovering how the ionosphere behaves and what processes shape it [*Hanson et al.*, 1977; *Chen et al.*, 1978;

[1]Department of Astronomy, Boston University, Boston, Massachusetts, USA.
[2]Institut für Raumfahrttechnik, Universität der Bundeswehr München, Munich, Germany.
[3]Electrical Engineering Department, Stanford University, Stanford, California, USA.
[4]Department of Physics and Astronomy, University of Iowa, Iowa City, Iowa, USA.
[5]Rheinisches Institut für Umweltforschung, University of Cologne, Cologne, Germany.
[6]CAAUL, Lisbon, Portugal.
[7]ESTEC, ESA, Noordwijk, Netherlands.

Corresponding author: Z. Girazian, Department of Astronomy, Boston University, 725 Commonwealth Ave., Boston, MA 02215, USA. (zrjg@bu.edu)

Barth et al., 1992; *Fox and Yeager*, 2006; *Withers*, 2009; *Mendillo et al.*, 2011].

[3] Since 2004, the Mars Express (MEX) Radio Science Experiment MaRS has used radio occultations to measure over five hundred vertical profiles of dayside ionospheric electron density from ∼60 km to ∼800 km altitude with a vertical resolution of 0.5 km and a measurement uncertainty that is usually $0.5–1.0 \times 10^9$ m^{-3} [*Pätzold et al.*, 2004, 2005]. Here we discuss the unprecedentedly clear view of the vertical structure of the Martian ionosphere that is provided by their excellent measurement accuracy, vertical range, and vertical resolution. We report diverse conditions in the topside ionosphere, atypical shapes of the main plasma layer, and new features above and below the main plasma layer.

[4] Previous work has established that the vertical structure of the dayside Martian ionosphere consists of a photochemically-controlled region (80–200 km) and a transport-controlled region (>200 km) [*Chen et al.*, 1978; *Barth et al.*, 1992; *Shinagawa*, 2000; *Fox*, 2004]. The most abundant ion below 300 km is O_2^+ [*Hanson et al.*, 1977; *Chen et al.*, 1978; *Fox*, 2004]. Interaction of the solar wind with the ionosphere generally produces an upper boundary separating electrons of Martian origin from those of solar origin [*Brain*, 2006; *Nagy et al.*, 2004, and references therein]. The typical altitude of this boundary, which varies considerably with time, is 400 km [*Mitchell et al.*, 2001; *Brain*, 2006; *Duru et al.*, 2009]. Maximum electron densities occur within the photochemically-controlled region in a plasma layer produced by solar EUV irradiance, called the M2 layer [*Fox and Yeager*, 2006; *Withers*, 2009]. A smaller, highly time-variable layer produced by solar soft X-ray irradiance and associated electron impact ionization, called the M1 layer, occurs about 20 km below the M2 layer [*Fox*, 2004; *Mendillo et al.*, 2006; *Withers*, 2009]. Electron densities above the M2 layer in the transport-controlled topside generally decrease with increasing altitude [*Hanson et al.*, 1977; *Zhang et al.*, 1990; *Fox and Yeager*, 2006; *Duru et al.*, 2009; *Mendillo et al.*, 2011]. Figure 1a shows such an electron density profile. The M1 layer is visible at 110 km, the M2 layer at 135 km has a classical Chapman-like shape [*Withers*, 2009], and electron densities decrease exponentially above the M2 layer. The exponential decrease in electron density by two orders of magnitude over 150 km distance has a single scale height of 33 km. We truncate all profiles shown in this paper at the first negative electron density measurement above the M2 layer.

2. The Topside Ionosphere

[5] In only 10% of profiles do topside electron densities clearly decrease with a single scale height. The topside of the profile in Figure 1b, like 25% of profiles, has two scale

heights, here 22 km from 150 to 220 km altitude and 120 km from 220 to 400 km altitude. Another 10% of profiles have three regions with distinct scale heights (Figure 1c: 28 km at 150–220 km, 190 km at 220–280 km, and 21 km at 280–315 km). Figure 1c is a rare Mars radio occultation profile that measures plasma above and below the ionopause (~300 km). Topside plasma scale heights are affected by ion and electron temperatures, large-scale plasma flow,
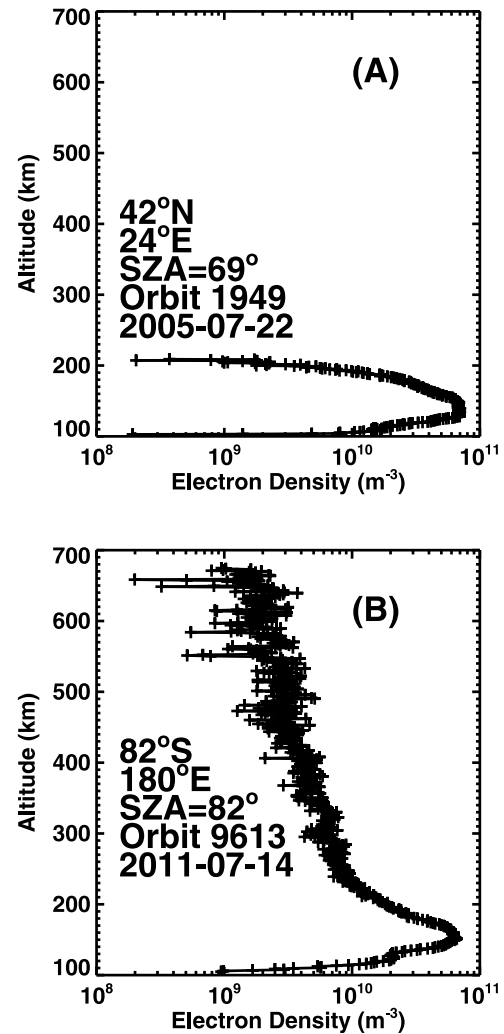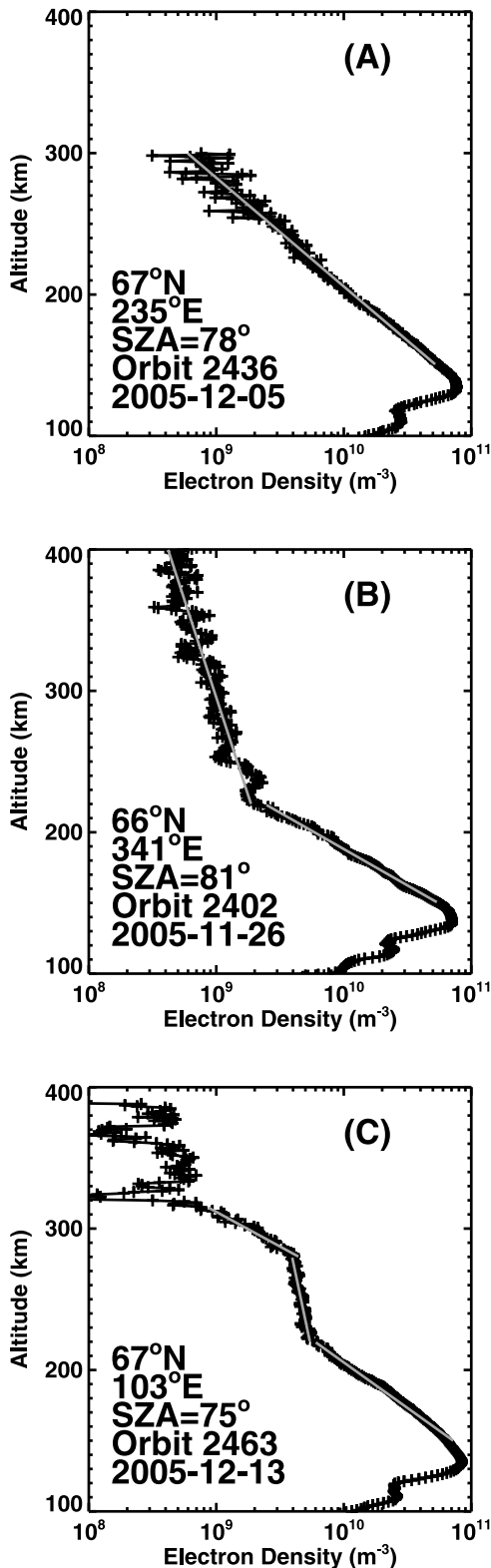
and the magnetic environment [*Schunk and Nagy*, 2009]. Abrupt transitions between regions of nearly-uniform plasma scale height suggest transitions in either the physical mechanism that controls the topside scale height (e.g., diffusive equilibrium, suppression of vertical flow by horizontal magnetic fields) or a key parameter for the dominant physical mechanism (e.g., ion composition, electron temperature, magnetic field strength). Extended regions with a nearly-uniform plasma scale height indicate that the dominant physical

Figure 1. Three electron density profiles illustrating *different structures in* the topside ionosphere. Latitude, longitude, solar zenith angle (SZA), orbit number, and UTC date are shown. All local times are 12–14 hours. (a) The grey solid line is an exponential fit to densities between 150 km and 300 km that has a scale height of 33 km. (b) The lower and upper grey solid lines are exponential fits to densities at 150–220 km and 220–400 km, respectively, that have scale heights of 22 km and 120 km. (c) The lower, middle, and upper grey solid lines are exponential fits to densities at 150–220 km, 220–280 km, and 280–315 km, respectively, that have scale heights of 28 km, 190 km, and 21 km.
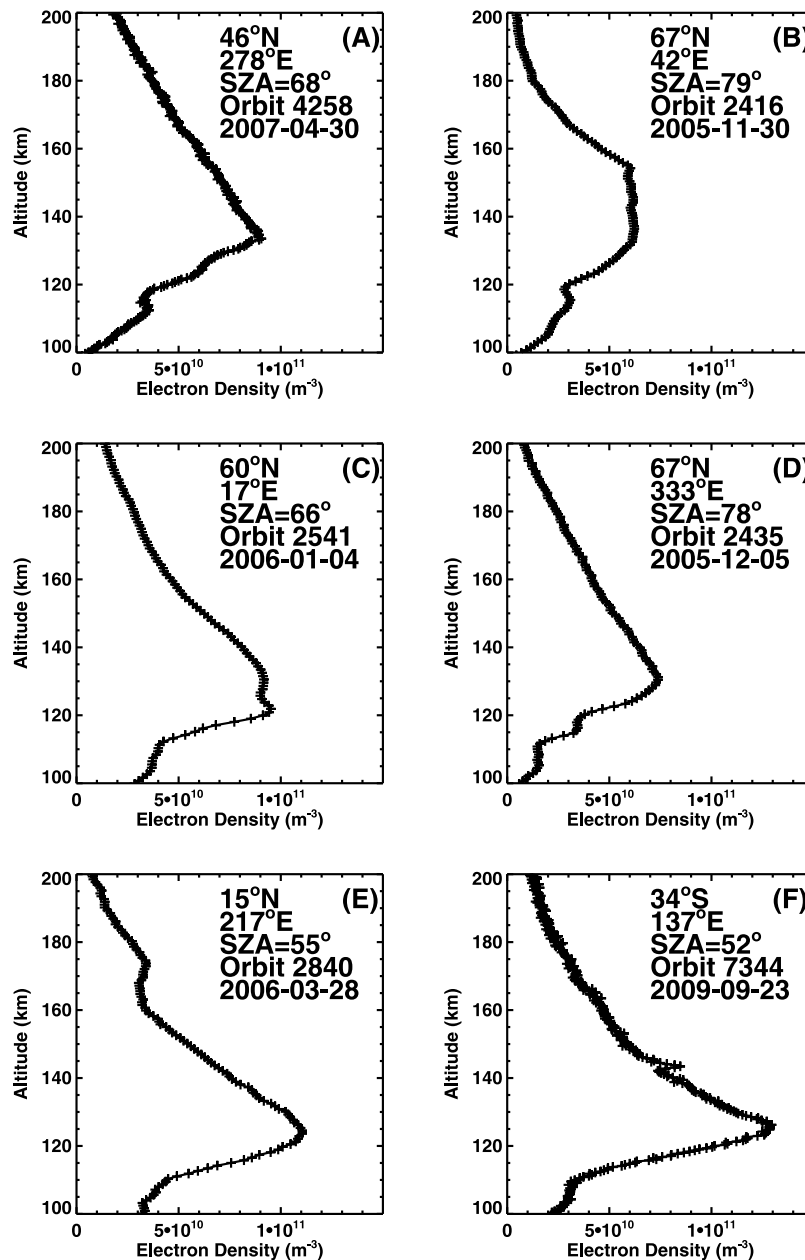

Figure 2. Two electron density profiles illustrating variations in the vertical extent of the ionosphere. The local time is (a) 11 hrs and (b) 21 hrs in Panel B.

Figure 3. Six electron density profiles illustrating atypical features near the main peak. All local times are within a few hours of local noon.

mechanism and its key parameters remain the same despite large changes in altitude.

[6] The height of the top of the ionosphere is not fixed, as shown in Figures 2a and 2b. In 25% of profiles, densities drop below 10^9 m^{-3} below 250 km, and in 1%, densities remain above 10^9 m^{-3} until 650 km. A cause of the unusually low extent and clear ionopause in Figure 2a was intense solar activity (i.e., temporal variability). Numerous coronal mass ejections occurred at this time and the fluxes of solar energetic particles at Earth and Mars were high [*Morgan et al.*, 2006]. A cause of the unusually high extent in Figure 2b was the strong, 220 nT at 150 km [*Arkani-Hamed*, 2004], and nearly horizontal crustal magnetic field at this location (i.e., spatial variability) that held off the solar wind. The vertical profile of electron density in Figure 2b has the greatest range yet reported for Mars, 600 km. The

vertical thickness of the ionosphere changes by a factor of six between Figure 2a (100 km thick) and Figure 2b (600 km thick).

[7] Figures 1 and 2 illustrate extreme spatial and temporal variations in the extent and morphology of the topside ionosphere, which is an important reservoir of escaping volatiles, with space and time. They highlight the difficulties inherent in developing an understanding of present-day volatile loss from Mars that adequately captures time-dependent changes in the space environment above Mars and position-dependent magnetic field variations across Mars.

3. The Main Ionospheric Layer

[8] The main ionospheric peak usually has a smooth shape similar to a classical Chapman layer (Figure 1a) [*Withers*

and Mendillo, 2005; *Morgan et al.*, 2008]. However, MEX observations show that the shape of the M2 layer can be substantially different from this ideal. The three examples in Figures 3a–3c display sharply pointed, flat-topped, and wavy shapes, respectively. These shapes occur in 5%, 6%, and 8% of profiles, respectively. The density maximum at 120 km in Figure 3c that lies below a wide dense layer of plasma is consistent with a commonly observed feature in MARSIS ionospheric sounding ionograms: a brief continuation of the ionospheric trace beyond the cusp at the peak frequency of the plasma layer [*Kopf et al.*, 2008, Figure 5a]. Figure 3d shows a new feature at 120 km between the M1 layer at 110 km and the M2 layer at 130 km. This feature, found in 3% of profiles, is also present in Figure 3a. Both Figures 3a and 3d share an unusual attribute in their topside ionospheres; their electron densities decrease linearly, not exponentially, with increasing altitude. The localized features seen in Figures 3a–3d may be influenced by a range of small-scale plasma instabilities that are important in the analogous E-region of the terrestrial ionosphere [*Kelley*, 2009]. As-yet-unidentified spatial or temporal variations in ionospheric chemistry are another potential cause. Figures 3a–3d illustrate that much remains to be learned about the photochemically-controlled ionospheric regions that contain most of the plasma present in the ionosphere and which were thought to be well-understood. It is not clear whether the root causes of these atypical features lie in ionospheric chemistry, dynamics, or energetics.

[9] The general trend in electron densities between the main peak and ∼200 km is an exponential decrease with increasing altitude. Electron densities in the 160–180 km range are enhanced above this trend in 10% of profiles. In Figure 3e, the enhancement is sufficient to cause a local maximum in electron density. This bulge is the "second layer" present near 180 km in about half of Mars Express topside radar sounder MARSIS observations [*Kopf et al.*, 2008]. Several numerical models have predicted the existence of this bulge, but for two different physical reasons. *Shinagawa and Cravens* [1992] associated it with converging vertical plasma motion affected by magnetic fields. *Fox and Yeager* [2006] associated it with a sharp increase in electron temperature, which reduces plasma neutralization rates, at these altitudes.

[10] The ionosphere of Mars is affected by the planet's unique magnetic environment. *Nielsen et al.* [2007] and *Gurnett et al.* [2008] reported elevated peak and topside electron densities, respectively, above regions of strong and vertical field. These effects are caused by increased plasma production and/or heating in regions where the solar wind plasma impinges directly onto the ionosphere. The crustal magnetic field strength at 150 km in Figure 3F's profile is 250 nT [*Arkani-Hamed*, 2004]. Electron densities in a 3 km-wide region are increased above the background trend by 20%. Similar features are present in 1% of profiles and have also been observed in strongly magnetized regions by other instruments at Mars [*Withers et al.*, 2005]. The localization in altitude of this feature has two possible interpretations. First, this feature is actually a narrow plasma layer at 145 km. Since plasma production by precipitating particles cannot be concentrated like this, such a magnetically-controlled feature must be produced by either small-scale or large-scale plasma motion within the ionosphere. Second, this feature is the consequence of the assumption of

horizontal uniformity in the processing of radio occultation data and horizontal variations in plasma density across a region where the magnetic field environment varies, as observed by *Nielsen et al.* [2007] and *Gurnett et al.* [2008]. Violations of this assumption may also impact some of the other results of this work.

4. Conclusions

[11] These Mars Express radio occultation measurements of vertical profiles of ionospheric electron density reveal a rich and complex range of features in the vertical structure of the ionosphere of Mars. Single, double, and triple scale height topsides occur in 10%, 25%, and 10% of profiles, respectively. Sharply pointed (5%), flat-topped (6%), and wavy (8%) shapes are sometimes found in the main layer, all features that indicate major departures from conditions in models that produce a Chapman-like shape. A broad increase in electron density at 160–180 km occurs in 10% of profiles and a narrow increase at similar altitudes, associated with strong magnetic fields, is found in 1% of profiles. An additional layer is present between the M1 and M2 layers in 3% of profiles. This array of features challenges numerical models, and accurately reproducing them will determine key ionospheric chemical, dynamical, and thermal properties.

References

Arkani-Hamed, J. (2004), A coherent model of the crustal magnetic field of Mars, *J. Geophys. Res.*, *109*, E09005, doi:10.1029/2004JE002265.
Barth, C. A., A. I. F. Stewart, S. W. Bougher, D. M. Hunten, S. J. Bauer, and A. F. Nagy (1992), Aeronomy of the current Martian atmosphere, in *Mars*, edited by H. H. Kieffer, B. M. Jakosky, C. W. Snyder, and M. S. Matthews, pp. 1054–1089, Univ. Arizona Press, Arizona.
Brain, D. A. (2006), Mars Global Surveyor measurements of the Martian solar wind interaction, *Space Sci. Rev.*, *126*, 77–112, doi:10.1007/s11214-006-9122-x.
Chen, R. H., T. E. Cravens, and A. F. Nagy (1978), The Martian ionosphere in light of the Viking observations, *J. Geophys. Res.*, *83*, 3871–3876.
Connerney, J. E. P., M. H. Acuña, P. J. Wasilewski, G. Kletetschka, N. F. Ness, H. Rème, R. P. Lin, and D. L. Mitchell (2001), The global magnetic field of Mars and implications for crustal evolution, *Geophys. Res. Lett.*, *28*, 4015–4018, doi:10.1029/2001GL013619.
Duru, F., D. A. Gurnett, R. A. Frahm, J. D. Winningham, D. D. Morgan, and G. G. Howes (2009), Steep, transient density gradients in the Martian ionosphere similar to the ionopause at Venus, *J. Geophys. Res.*, *114*, A12310, doi:10.1029/2009JA014711.
Fox, J. L. (2004), Advances in the aeronomy of Venus and Mars, *Adv. Space Res.*, *33*, 132–139.
Fox, J. L., and K. E. Yeager (2006), Morphology of the near-terminator Martian ionosphere: A comparison of models and data, *J. Geophys. Res.*, *111*, A10309, doi:10.1029/2006JA011697.
Gurnett, D. A., et al. (2008), An overview of radar soundings of the Martian ionosphere from the Mars Express spacecraft, *Adv. Space Res.*, *41*, 1335–1346, doi:10.1016/j.asr.2007.01.062.
Hanson, W. B., S. Sanatani, and D. R. Zuccaro (1977), The Martian ionosphere as observed by the Viking retarding potential analyzers, *J. Geophys. Res.*, *82*, 4351–4363.

Kelley, M. C. (2009), *The Earth's Ionosphere: Plasma Physics and Electrodynamics, Second Edition*, Academic Press., Waltham, Mass.

Kopf, A. J., D. A. Gurnett, D. D. Morgan, and D. L. Kirchner (2008), Transient layers in the topside ionosphere of Mars, *Geophys. Res. Lett.*, *35*, L17102, doi:10.1029/2008GL034948.

Mendillo, M., P. Withers, D. Hinson, H. Rishbeth, and B. Reinisch (2006), Effects of solar flares on the ionosphere of Mars, *Science*, *311*, 1135–1138, doi:10.1126/science.1122099.

Mendillo, M., A. Lollo, P. Withers, M. Matta, M. Pätzold, and S. Tellmann (2011), Modeling Mars' ionosphere with constraints from same-day observations by Mars Global Surveyor and Mars Express, *J. Geophys. Res.*, *116*, A11303, doi:10.1029/2011JA016865.

Mitchell, D. L., R. P. Lin, C. Mazelle, H. Rème, P. A. Cloutier, J. E. P. Connerney, M. H. Acuña, and N. F. Ness (2001), Probing Mars' crustal magnetic field and ionosphere with the MGS Electron Reflectometer, *J. Geophys. Res.*, *106*, 23,419–23,428.

Morgan, D. D., D. A. Gurnett, D. L. Kirchner, R. L. Huff, D. A. Brain, W. V. Boynton, M. H. Acuña, J. J. Plaut, and G. Picardi (2006), Solar control of radar wave absorption by the Martian ionosphere, *Geophys. Res. Lett.*, *33*, L13202,doi:10.1029/2006GL026637.

Morgan, D. D., D. A. Gurnett, D. L. Kirchner, J. L. Fox, E. Nielsen, and J. J. Plaut (2008), Variation of the Martian ionospheric electron density from Mars Express radar soundings, *J. Geophys. Res.*, *113*, A09303, doi:10.1029/2008JA013313.

Nagy, A. F., et al. (2004), The plasma environment of Mars, *Space Sci. Rev.*, *111*, 33–114, doi:10.1023/B:SPAC.0000032718.47512.92.

Nielsen, E., D. D. Morgan, D. L. Kirchner, J. Plaut, and G. Picardi (2007), Absorption and reflection of radio waves in the Martian ionosphere, *Planet. Space Sci.*, *55*, 864–870, doi:10.1016/j.pss.2006.10.005.

Pätzold, M., et al. (2004), *MaRS: Mars Express Orbiter Radio Science*, *Eur. Space Agency Spec. Publ. ESA SP-1240*, 141–163.

Pätzold, M., S. Tellmann, B. Häusler, D. Hinson, R. Schaa, and G. L. Tyler (2005), A sporadic third layer in the ionosphere of Mars, *Science*, *310*, 837–839, doi:10.1126/science.1117755.

Schunk, R. W., and A. F. Nagy (2009), *Ionospheres*, 2nd ed., Cambridge Univ. Press, New York.

Shinagawa, H. (2000), Our current understanding of the ionosphere of Mars, *Adv. Space Res.*, *26*, 1599–1608.

Shinagawa, H., and T. E. Cravens (1992), The ionospheric effects of a weak intrinsic magnetic field at Mars, *J. Geophys. Res.*, *97*, 1027–1035.

Withers, P. (2009), A review of observed variability in the dayside ionosphere of Mars, *Adv. Space Res.*, *44*, 277–307, doi:10.1016/j.asr.2009.04.027.

Withers, P., and M. Mendillo (2005), Response of peak electron densities in the Martian ionosphere to day-to-day changes in solar flux due to solar rotation, *Planet. Space Sci.*, *53*, 1401–1418, doi:10.1016/j.pss.2005.07.010.

Withers, P., M. Mendillo, H. Rishbeth, D. P. Hinson, and J. Arkani-Hamed (2005), Ionospheric characteristics above Martian crustal magnetic anomalies, *Geophys. Res. Lett.*, *32*, L16204, doi:10.1029/2005GL023483.

Zhang, M. H. G., J. G. Luhmann, A. J. Kliore, and J. Kim (1990), A post-Pioneer Venus reassessment of the Martian dayside ionosphere as observed by radio occultation methods, *J. Geophys. Res.*, *95*, 14,829–14,839.